Robustness of the scanning second harmonic generation microscopy technique for characterization of hotspot patterns in plasmonic nanomaterials

V. K. Valev[1,*], B. De Clercq[2], X. Zheng[3], C. G. Biris[4], N. C. Panoiu[4], A. V. Silhanek[5], V. Volskiy[3], O. A. Aktsipetrov[6,†], G. A. E. Vandenbosch[3], M. Ameloot[2], V. V. Moshchalkov[7], T. Verbiest[1]

[1] Molecular Electronics and Photonics, INPAC, KU Leuven, Celestijnenlaan 200 D, B-3001 Leuven, Belgium
[2] University Hasselt and transnational University Limburg, BIOMED, Agoralaan building C, B-3590, Diepenbeek, Belgium
[3] ESAT-TELEMIC, KU Leuven, B-3001 Leuven, Belgium
[4] Department of Electronic and Electrical Engineering, University College London, Torrington Place, London, WC1E 7JE, United Kingdom
[5] Département de Physique, Université de Liège, Bât. B5, Allée du 6 août, 17, B-4000 Sart Tilman, Belgium
[6] Department of Physics, Moscow State University, 11992 Moscow, Russia
[7] Nanoscale Superconductivity and Magnetism & Pulsed Fields Group, INPAC, Katholieke Universiteit Leuven, Celestijnenlaan 200 D, B-3001 Leuven, Belgium
*Corresponding author: v.k.valev@fys.kuleuven.be

ABSTRACT

Scanning second harmonic generation (SHG) microscopy is becoming an important tool for characterizing nanopatterned metal surfaces and mapping plasmonic local field enhancements. Here we study G-shaped and mirror-G-shaped gold nanostructures and test the robustness of the experimental results versus the direction of scanning, the numerical aperture of the objective, the magnification, and the size of the laser spot on the sample. We find that none of these parameters has a significant influence on the experimental results.

Keywords: Second Harmonic Generation, metamaterials, nanostructures, plasmonics

INTRODUCTION

In the last ten years, there has been a remarkable increase of interest in plasmonic nanomaterials.[1,2,3] These materials, which can support coherent oscillations of surfaces charges, have been associated with revolutionary new applications, such as invisibility,[4] negative refraction[5,6,7] or super-lensing.[8,9] Because nanostructures exhibit a very large surface-to-volume ratio and because surface-plasmons are readily excited with optical radiation, their study can greatly benefit from a surface-sensitive optical technique, such as second harmonic generation (SHG).

SHG is a nonlinear optical mechanism, whereby two photons with the same energy are converted into a single photon having twice as much energy. The mechanism occurs via virtual energy levels and does not require the presence of specific resonances. For this reason, the SHG technique constitutes a very general

[†] Regretfully, Prof. Oleg A. Aktsipetrov passed away in the autumn of 2011.

Nanophotonics IV, edited by David L. Andrews, Jean-Michel Nunzi, Andreas Ostendorf,
Proc. of SPIE Vol. 8424, 842411 · © 2012 SPIE · CCC code: 0277-786X/12/$18
doi: 10.1117/12.922880

and powerful investigation tool. Moreover, within the dipole approximation, SHG is forbidden in centrosymmetric materials, i.e. it is only allowed in the case of symmetry breaking. Symmetry breaking is observed, for instance, at surfaces and interfaces of materials and, indeed, SHG exhibits surface/interface sensitivity down to the atomic monolayer.[10] Additionally, SHG has been successfully employed to study symmetry breaking phenomena, such as externally applied electric[11] or magnetic[12] dc fields, though care should be taken while estimating the latter.[13] SHG can also provide contrast for imaging ferroelectric[14] and ferromagnetic[15] domains.

In the case of nanostructured materials, the coupling of incident radiation to surface-plasmons leads to local field enhancements that can greatly influence the SHG response. SHG has thus successfully been employed for the detection of single plasmonic particles.[16,17] Additionally, plasmonic coupling,[18,19,20] propagation of plasmons along a chain of particles[21,22,23] and propagating plasmons scattered by metallic nanoparticles[24] can be probed by SHG. The SHG technique is also very sensitive to further symmetry breaking in the plasmonic nanomaterials. Externally applying a magnetic field to nickel nanostructures has been studied,[25] as well as chiral symmetry breaking.[26] The latter has particularly been studied through the circular dichroism effect.[27,28,29] In order to account for the influence of local field enhancements in the SHG signal from nanomaterials, several theoretical models have recently been developed.[30,31,32,33,34,35]

In combination with microscopy, SHG can provide an accurate mapping of local field enhancements at the surface of nanomaterials.[36,37,38] More specifically, the local field enhancements can be visualized as hotspots.[39] Furthermore, for sufficiently high incoming light intensity, it has been demonstrated that these hotspots can be imprinted onto the surface of the nanostructures themselves through nanobump and nanojet formation.[40,41] SHG microscopy is therefore becoming a very important tool for studying plasmonic nanomaterials. In this context, it is worth examining the influence of the various microscope specific parameters on the hotspot pattern.

Here, we examine the influence of the scanning direction, numerical aperture of the objective, magnification, and the laser spot size on the second harmonic generation pattern of hotspots. The sample we have studied consist of chiral G-shaped gold nanostructures.[42] We demonstrate that none of these parameters significantly affects the results.

EXPERIMENTS

The samples consists of G-shaped and mirror-G-shaped gold nanostructures (25 nm thick) deposited by electron beam lithography on substrates composed of SiO_2 (100 nm thick) placed on top of a Si(001) wafer. The G-shaped and mirror-G-shaped nanostructures are arranged in unit cells composed of four Gs (or mirror-Gs), each rotated 90° with respect to its neighbors. The separation distance between the Gs (or mirror-Gs) is 200 nm. The Gs (or mirror-Gs) themselves are 1 μm large, with line width 200 nm. More details regarding the sample preparation can be found in Ref. [43].

Scanning second harmonic generation microscopy is performed by adapting a commercial scanning confocal microscope. During measurements the laser spot is scanned at adjustable speed and direction over the sample surface. The illumination itself is performed by means of a pulsed Ti:Sapphire laser, with 800 nm wavelength. In the case of the 100x objective with numerical aperture (NA) of 1.46, the spot size on the sample is approximately 400 nm in diameter. Further details regarding the microscope configuration and procedure can be found in Ref. [44].

RESULTS

Numerical simulations of the electrical currents at the fundamental frequency in the G-shaped nanostructures were performed with the MAGMAS software, see Fig. 1a. MAGMAS is a numerical software tool, originally developed at the KU Leuven, for electromagnetic problems in the microwave and millimeter wave frequency bands.[45,46] It has been extended to include the special features of plasmonic nanotechnology: (near) optical frequencies, strongly dispersive materials and the need for volumetric meshing. More specifically, Fig. 1a illustrates the distribution of local currents at the surface of the

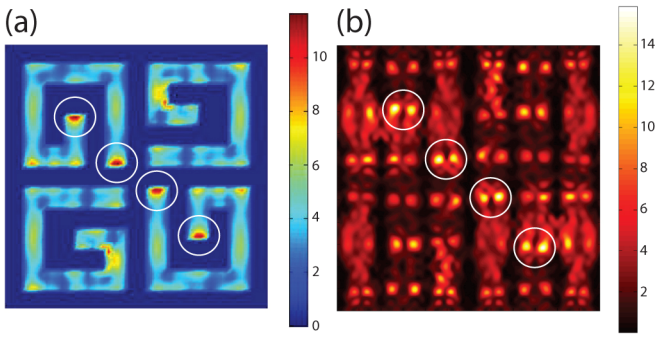

Fig.1. In (a), the density of local electric currents at the surface of the nanostructures. In (b), the squared amplitude of electric near-fields at the surface of the nanostructures.

nanostructures. Four hotspots oriented along the main diagonal of the unit cell can clearly be identified. For the sake of completeness, numerical simulations of the electric near-fields at the fundamental frequency were also performed, using RSoft's Diffract MOD software, see Fig. 1b. The code implements a numerical

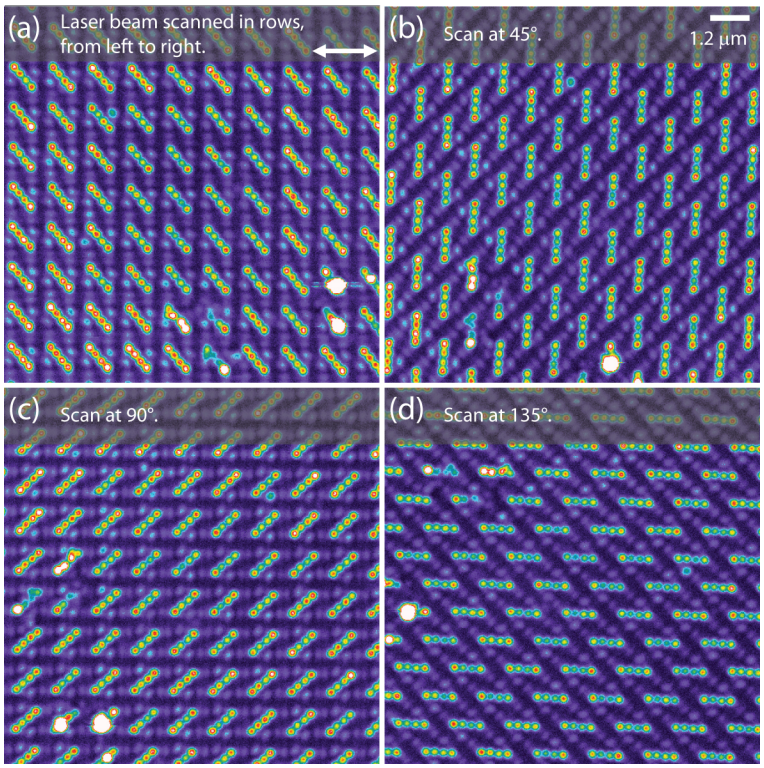

Fig.2. Scanning Second Harmonic Generation microscopy of G-shaped gold nanostructures shows that the pattern of hotspots is independent from the scanning direction. A 100x objective with NA=1.46 was used. In (a), the nanostructured array is scanned in rows, from left to right. The direction of polarization is indicated by the white arrow. In (b), the array is scanned along the diagonal, i.e. at 45°. In (c), the array is scanned from top to bottom, i.e. at 90°. In (d), the array is scanned along the other diagonal, i.e. at 135°. Regardless of the scanning direction, the hotspot pattern remains the same, being only rotated.

method widely used in the analysis of optical properties of metallic and dielectric diffraction gratings, namely, the rigorous coupled-wave analysis method. The results shown in Fig. 1b are in remarkable agreement with those in Fig. 1a – four hotspots are clearly distinguishable and they are oriented along the main diagonal of the unit cell.

Figure 2 shows the dependence of the SHG signal on the direction of scanning. To gather the data presented in Fig. 2a, the laser beam is scanned in rows, from left to right. The incident light is linearly polarized along the horizontal direction as it is indicated with the white arrow. The hotspot pattern in the unit cells is composed of four hotspots oriented along the main diagonal. The color coded intensities follow the rainbow color order, starting from violet and finishing with white. The latter color usually indicates saturation of the detector. Upon rotating the direction of scanning by 45°, the orientation of the hotspots changes accordingly, as can be seen in Fig. 2b. Rotating the scan by 90° and 135° also results in a corresponding hotspot orientation change; these changes can be seen in Fig. 2c and 2d, respectively. Figure 2 demonstrates that besides the expected variation in the orientation of the hotspots, the hotspot pattern itself is not affected by the scanning direction. In other words, the SHG hotspot pattern does not depend on the scanning procedure.

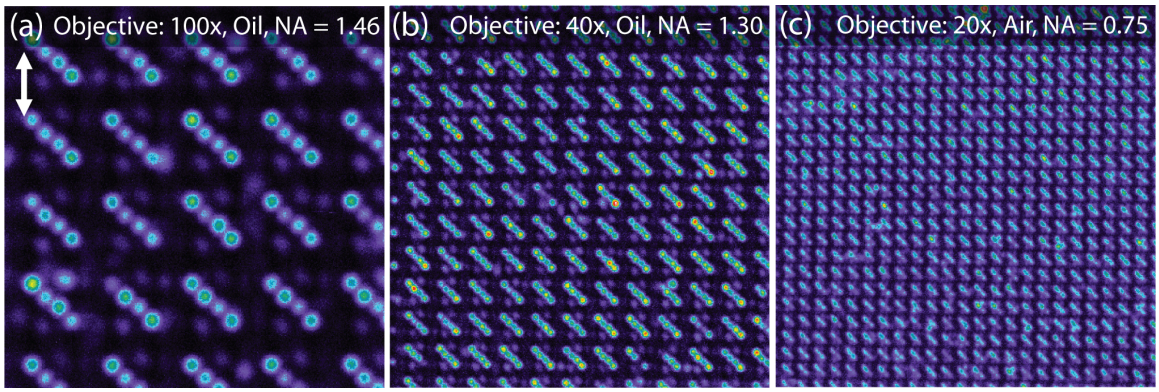

Fig.3. Scanning Second Harmonic Generation microscopy of mirror-G-shaped gold nanostructures depending on the magnification and the numerical aperture (NA) of the microscope objective. In (a), upon using a 100x objective with NA=1.46, a clear hotspot pattern, composed of four bright spots along the diagonal, can be seen. In (b), a micrograph that was obtained with a 40x objective, NA=1.3. In (c), a micrograph that was obtained with 20x magnification objective having NA=0.75. With decreasing magnification and NA, the pattern of hotspots remains essentially the same. The direction of polarization is indicated by the white arrow.

In Figure 3, the robustness of the SHG hotspot pattern is tested against variations of the magnification, numerical aperture, and the size of the focal spot on the sample. To show that these results are valid regardless of the chirality in the sample, we now turn our attention to the mirror-G geometry. In order to make the data easily comparable to those in Fig. 2a, we rotate the direction of linearly polarized light by 90°. The combination of 90° rotated polarization and mirror image of the unit cell yields a pattern of hotpots that are again oriented along the main diagonal. In Fig. 3a, we show a micrograph that was obtained with a 100x oil objective with NA=1.46. For this numerical aperture and for linearly polarized light the spot at the focus is an ellipse with semi-axes of 440 nm and 330 nm. These dimensions are clearly smaller than the size of Gs, which is 1 μm. As can be seen in Fig. 3a, the hotspot pattern is similar to that in Fig. 3a, except for the fact that it is less intense. The reason for this is that we used less laser power, to avoid saturating the detector. Next, an image was made using a 40x oil objective with NA=1.3; this image can be seen in Fig. 3b. Although the magnification is significantly smaller, the pattern of four hotspots in each unit cell is still clearly distinguishable. Figure 3c presents a micrograph that was taken with a 20x air objective

with NA=0.75. At this low magnification, the four individual hotspots are no longer resolved, yet the general local field enhancement in each unit cell is clearly reproduced. Because the spot size at the focus scales with the numerical aperture, in Fig. 3c the spot size is approximately two times as large as that in Fig. 3a. We can therefore conclude that the pattern of SHG hotspots is not significantly affected by the magnification of the objective, the numerical aperture or the laser spot size in focus of the sample.

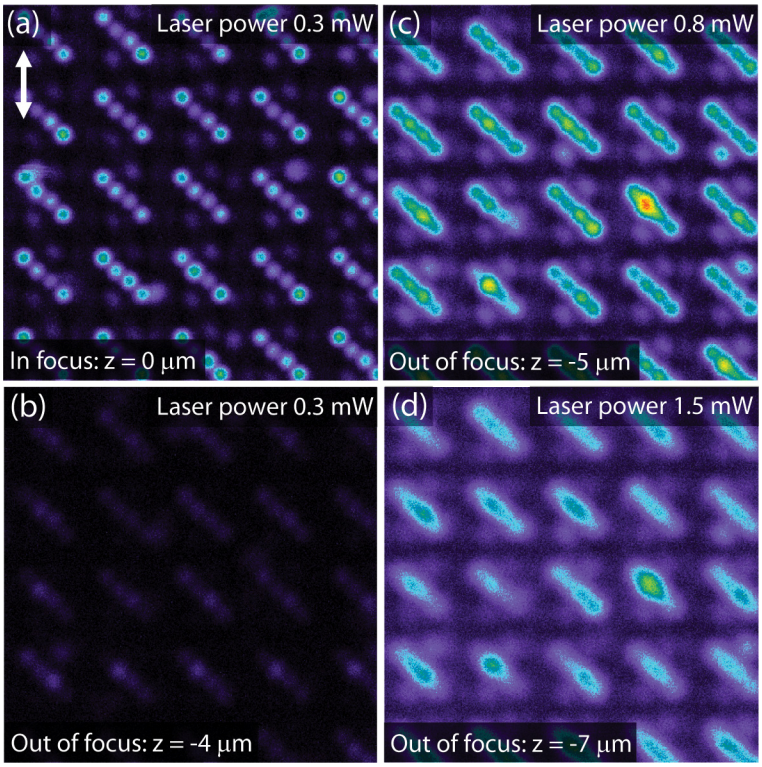

Fig.4. Scanning Second Harmonic Generation Microscopy of mirror-G-shaped gold nanostructures dependence on defocusing. In (a), the image is in focus (Z=0) and the laser power is 0.3 mW. In (b), for same laser power, defocusing the pictures by 4 μm leads to a dramatic loss of hotspot intensity. In (c), the hotspot intensity in the defocused image can be recovered by increasing the incident laser power to 0.8 mW. In (d), a hotspot pattern can still be distinguished upon defocusing by 7μm , for incident laser power of 1.5 mW. Although the images are defocused, the pattern of hotspots remains essentially the same, only the image becomes blurry, i.e. out of focus. The direction of polarization is indicated by the white arrow.

The dependence of the SHG image on laser spot size at the sample can also be investigated by defocusing the light. Figure 4a shows a SHG micrograph that was obtained for vertical linearly polarized light illuminating the mirror-G-shaped nanostructures. The microscope objective used was the 100x oil objective with NA=1.46. The color-coded intensities evolve from black, through purple, blue, green and yellow to red. The picture is at the focus, i.e. the microscope objective is positioned at z = 0 μm, and the illumination intensity is 0.3 mW. Moving away from focus increases the spot size and consequently there is a drop in the SHG signal. This is illustrated in Fig. 4b, where the objective is positioned at z = -4 μm for the same laser power. The figure shows that the pattern of hotpots is barely visible. The SHG intensity from the hotspots can be recovered though by increasing the incident laser power, see Fig. 4c. Indeed, upon positioning the objective at z = -5 μm, increasing laser power to 0.8 mW allows the visualization of the four individual hotspots in each unit cell. Further defocusing (z = - 7 μm) with laser power of 1.5 mW does

not resolve the individual hotspots, although the general trend is still clear. Consequently, Fig. 4 demonstrates that, in this case, increasing the laser spot size on the sample by the defocusing the objective does not significantly affect the pattern of SHG hotspots.

CONCLUSION

We have examined the effect of varying the scanning direction, magnification, numerical aperture, and the laser spot size on the SHG hotspots pattern produced by scanning SHG microscopy. We find that the SHG results are robust against varying these parameters. Our findings are of particular importance not only for scanning SHG but also for the general use of scanning microscopy techniques for the purpose of imaging or manipulating local field enhancements.[47]

ACKNOWLEDGEMENTS

We acknowledge financial support from the Fund for scientific research Flanders (FWO-V), the K.U. Leuven (CREA, GOA), Methusalem Funding by the Flemish government and the Belgian Inter-University Attraction Poles IAP Programmes. V.K.V., is grateful for the support from the FWO-Vlaanderen. B. DC. is thankful to the IWT. O.A.A. is partly supported by the Russian Foundation for Basic Research. M.A. recognizes the Province of Limburg (Belgium) for the financial support within the tUL IMPULS FASE II program allowing for the upgrading the laser source used in this work.

REFERENCES

[1] Novotny L. and Hecht, B. [Principles of Nano-Optics], Cambridge University Press, Cambridge, (2006).
[2] Rigneault, H., Lourtioz, J.M., Delalande, C. and Levenson, A. [Nanophotonics], eds. ISTE, London, (2006)
[3] edited by Brongersma, M. L. and Kirk, P. G., [Surface Plasmon Nanophotonics], Springer, Dordrecht, (2007).
[4] Schurig, D., Mock, J., J., Justice, B., J., Cummer, S., A., Pendry, J., B., Starr, A., F. and Smith, D., R., "Metamaterial Electromagnetic Cloak at Microwave Frequencies," Science 314, 977 (2006).
[5] Shelby, R.,A., Smith, D.,R. and Schultz, S. "Experimental Verification of a Negative Index of Refraction," Science 292, 5514 (2001).
[6] Pendry, J.,B. "Negative Refraction," Contemp. Phys. 45, 191 (2004).
[7] Veselago, V., G., "The electrodynamics of substances with simultaneously negative values of [permittivity] and [permeability]," Sov. Phy. Usp. 10, 509 (1968).
[8] Grbic, A. and Eleftheriades, G.,V. "Overcoming the Diffraction Limit with a Planar Left-Handed Transmission-Line Lens," Phys. Rev. Lett, 92, 117403 (2004).
[9] Fang, N., Lee, H., Sun, C. and Zhang, X., "Sub–Diffraction-Limited Optical Imaging with a Silver Superlens," Science 308, 534 (2005).
[10] Valev, V. K., Kirilyuk, A., Rasing, Th., Dela Longa, F., Kohlhepp, J. T. and Koopmans, B., "Oscillations of the net magnetic moment and magnetization reversal properties of the Mn/Co interface," Phys. Rev. B 75, 012401 (2007).
[11] Lee, C. H., Chang, R. K. and Bloembergen, N., "Nonlinear electroreflectance in silicon and silver," Phys. Rev. Lett. 18(5), 167–170 (1967).
[12] Kirilyuk, A. and Rasing, Th., "Magnetization-induced-second-harmonic generation from surfaces and interfaces," J. Opt. Soc. Am. B 22(1), 148–167 (2005).
[13] Valev, V. K., Gruyters, M., Kirilyuk, A. and Rasing, Th., "Influence of quadratic contributions in magnetization-induced second harmonic generation studies of magnetization reversal," Phys. Stat. Sol. (b) 242, 3027–3031 (2005).
[14] Sheng, Y., Best, A., Butt, H.-J., Krolikowski, W., Arie, A. and Koynov, K., "Three-dimensional ferroelectric domain visualization by Cerenkov-type second harmonic generation," Opt. Express 18(16), 16539–16545 (2010).
[15] Pavlov, V. V., Ferré, J., Meyer, P., Tessier, G., Georges, P., Brun, A., Beauvillain, P. and Mathet, V., "Linear and non-linear magneto-optical studies of Pt/Co/Pt thin films," J. Phys. Condens. Matter 13(44), 9867–9878 (2001).
[16] Butet,, J., Duboisset, J., Bachelier, G., Russier-Antoine, I., Benichou, E., Jonin, C. and Brevet, P.-F., "Optical Second Harmonic Generation of Single Metallic Nanoparticles Embedded in a Homogeneous Medium," Nano Lett. 10(5), 1717–1721 (2010).
[17] Butet, J., Bachelier, G., Duboisset, J., Bertorelle, F., Russier-Antoine, I., Jonin, C., Benichou, E. and Brevet, P.-F., "Three-dimensional mapping of single gold nanoparticles embedded in a homogeneous transparent matrix using optical second-harmonic generation," Opt. Express 18(21), 22314–22323 (2010).

[18] Benedetti, A., Centini, M., Sibilia, C. and Bertolotti, M., “Engineering the second harmonic generation pattern from coupled gold nanowires,” J. Opt. Soc. Am. B 27(3), 408–416 (2010).
[19] Centini, M., Benedetti, A., Sibilia, C. and Bertolotti, M., “Coupled 2D Ag nano-resonator chains for enhanced and spatially tailored second harmonic generation,” Opt. Express 19, 8218-8232 (2011).
[20] Belardini, A., Larciprete, M. C., Centini, M., Fazio, E., Sibilia, C., Bertolotti, M., Toma, A., Chiappe, D. and Buatier de Mongeot, F., “Tailored second harmonic generation from self-organized metal nano-wires arrays,” Opt. Express 17(5), 3603–3609 (2009).
[21] Biris, C.G. and Panoiu, N. C., "Excitation of dark plasmonic cavity modes via nonlinearly induced dipoles: applications to near-infrared plasmonic sensing," Nanotechnology 22, 235502 (2011).
[22] Biris, C. G. and Panoiu, N. C, "Excitation of linear and nonlinear cavity modes upon interaction of femtosecond pulses with arrays of metallic nanowires," Appl Phys A 103, 863–867 (2011).
[23] Awada, Ch., Kessi, F. , Jonin, Ch., Adam, P. M., Kostcheev, S., Bachelot, R., Royer, P., Russier-Antoine, I., Benichou, E., Bachelier, G. and Brevet, P. F., "On- and off-axis second harmonic generation from an array of gold metallic nanocylinders," J. Appl. Phys. 110, 023109 (2011).
[24] Cao, L., Panoiu, N. C. and Osgood, R. M., "Surface second-harmonic generation from surface plasmon waves scattered by metallic nanostructures," Phys. Rev. B 75, 205401 (2007).
[25] Valev, V. K., Volodin, A., Silhanek, A. V., Gillijns, W., De Clercq, B., Jeyaram, Y., Paddubrouskaya, H., Biris, C. G., Panoiu, N. C., Aktsipetrov, O. A., Ameloot, M., Moshchalkov, V. V. and Verbiest, T., "Plasmons reveal the direction of magnetization in nickel nanostructures," ACS Nano*,* 5, 91-96 (2011).
[26] Valev, V. K., Silhanek, A. V., Verellen, N., Gillijns, W., Vandenbosch, G.A.E., Aktsipetrov, O. A., Moshchalkov, V. V. and Verbiest, T., "Asymmetric Second Harmonic Generation from Chiral G-Shaped Gold Nanostructures," Phys. Rev. Lett.*,* 104, 127401 (2010).
[27] Valev, V. K., Smisdom, N., Silhanek, A. V., De Clercq, B., Gillijns, W., Ameloot, M., Moshchalkov, V. V. and Verbiest, T. "Plasmonic Ratchet Wheels: Switching Circular Dichroism by Arranging Chiral Nanostructures," Nano Lett. 9, 3945 (2009).
[28] Belardini, A., Larciprete, M. C., Centini, M., Fazio, E., Sibilia, C., Chiappe, D., Martella, C., Toma, A., Giordano, M. and Buatier de Mongeot, F., "Circular Dichroism in the Optical Second-Harmonic Emission of Curved Gold Metal Nanowires," Phys. Rev. Lett. 107, 257401 (2011) .
[29] Huttunen, M.J., Bautista, G., Decker, M., Linden, S., Wegener, M. and Kauranen, M., “Nonlinear chiral imaging of subwavelength-sized twisted-cross gold nanodimers," Opt. Mat. Express 1, 46–56 (2011).
[30] Cao, L., Panoiu, N. C., Bhat, R.D.R. and Osgood, R.M., “Surface second-harmonic generation from scattering of surface plasmon polaritons from radially symmetric nanostructures," Phys. Rev. B 79, 235416 (2009).
[31] Biris, C.G. and Panoiu, N.C., “Second harmonic generation in metamaterials based on homogeneous centrosymmetric nanowires," Phys. Rev. B 81, 195102 (2010).
[32] Dadap, J. I., Shan, J., Eisenthal, K. B. and Heinz, T. F., “Second-harmonic Rayleigh scattering from a sphere of centrosymmetric material,” Phys. Rev. Lett. 83(20), 4045–4048 (1999).
[33] Zeng, Y., Hoyer, W., Liu, J., Koch, S. W. and Moloney, J. V., “Classical theory for second-harmonic generation from metallic nanoparticles,” Phys. Rev. B 79(23), 235109 (2009).
[34] Schaich, W. L., “Second harmonic generation by periodically-structured metal surfaces,” Phys. Rev. B 78(19), 195416 (2008).
[35] Mäkitalo, J., Suuriniemi, S. and Kauranen, M., "Boundary element method for surface nonlinear optics of nanoparticles," Opt. Express 19, 23386 (2011).
[36] Zayats, A.V., Smolyaninov, I.I. and Davis, C.C., “Observation of localized plasmonic excitations in thin metal films with near-field second-harmonic microscopy," Optics Communications 169, 93–96 (1999).
[37] Anceau, C., Brasselet, S., Zyss, J. and Gadenne, P., “Local second-harmonic generation enhancement on gold nanostructures probed by two-photon microscopy," Opt. Lett. 28(9), 713–715 (2003).
[38] Valev, V. K., Silhanek, A. V., Smisdom, N., De Clercq, B., Gillijns, W., Aktsipetrov, O. A., Ameloot, M., Moshchalkov, V. V. and Verbiest, T., "Linearly Polarized Second Harmonic Generation Microscopy Reveals Chirality," Optics Express*,* 18, 8286-8293 (2010).
[39] Valev, V. K., Silhanek, A. V., De Clercq, B., Gillijns, W., Jeyaram, Y., Zheng, X., Volskiy, V., Aktsipetrov, O. A., Vandenbosch, G. A. E., Ameloot, M., Moshchalkov, V. V. and Verbiest, T., "U-shaped switches for optical information processing at the nanoscale," Small 7, 2573-2576 (2011).
[40] Valev, V. K., Silhanek, A. V., Jeyaram, Y., Denkova, D., De Clercq, B., Petkov, V., Zheng, X., Volskiy, V., Gillijns, W., Vandenbosch, G. A. E., Aktsipetrov, O. A., Ameloot, M., Moshchalkov, V. V. and Verbiest, T., "Hotspot decorations map plasmonic patterns with the resolution of scanning probe techniques," Phys. Rev. Lett. 106, 226803 (2011).
[41] Valev, V. K., Denkova, D., Zheng, X., Kuznetsov, A. I., Reinhardt, C., Chichkov, B. N., Tsutsumanova, G., Osley, E.J., Petkov, V., De Clercq, B., Silhanek, A. V., Jeyaram, Y., Volskiy, V., Warburton, P. A., Vandenbosch, G. A. E.,

Russev, S., Aktsipetrov, O. A., Ameloot, M., Moshchalkov, V. V. and Verbiest, T., "Plasmon-enhanced sub-wavelength laser ablation: plasmonic nanojets," Adv. Mater. 24, OP29-OP35 (2012).
[42] Mamonov, E. A., Murzina, T. V., Kolmychek, I. A., Maydykovsky, A. I., Valev, V. K., Silhanek, A. V., Ponizovskaya, E., Bratkovsky, A., Verbiest, T., Moshchalkov, V. V. and Aktsipetrov, O. A., "Coherent and incoherent second harmonic generation in planar G-shaped nanostructures," Opt. Lett. 36, 3681-3683 (2011).
[43] Valev, V. K., Zheng, X., Biris, C.G., Silhanek, A.V., Volskiy, V., De Clercq, B., Aktsipetrov, O.A., Ameloot, M., Panoiu, N.C., Vandenbosch, G. A. E. and Moshchalkov, V. V., "The Origin of Second Harmonic Generation Hotspots in Chiral Optical Metamaterials," Opt. Mater. Express 1, 36-45 (2011).
[44] Valev, V. K., De Clercq, B., Zheng, X., Denkova, D., Osley, E. J., Vandendriessche, S., Silhanek, A. V., Volskiy, V., Warburton, P. A., Vandenbosch, G. A. E., Ameloot, M., Moshchalkov, V. V. and Verbiest, T., "The role of chiral local field enhancements below the resolution limit of Second Harmonic Generation microscopy," Opt. Express 20, 256-264 (2012).
[45] Schols, Y. and Vandenbosch, G. A. E., "Separation of horizontal and vertical dependencies in a surface/volume integral equation approach to model quasi 3-D structures in multilayered media," IEE Proc Microw Antennas Propag., 55, 1086-1094 (2007).
[46] Vrancken, M. and Vandenbosch, G. A. E., "Hybrid dyadic-mixed potential integral equation analysis of 3D planar circuits and antennas," IEE Proc. Microwaves, Antennas Propagat., 149, 265-270 (2002).
[47] Dostert, K.H., Álvarez, M., Koynov, K., del Campo, A., Butt, H.J. and Kreiter, M., "Near Field Guided Chemical Nanopatterning," Langmuir 28, 3699-3703 (2012).